THERMOCHEMISTRY OF THE BINARY SYSTEM NITROCELLULOSE+2,6-DINITROTOLUENE

A. Książczak[1] and T. Wolszakiewicz[2]

[1]Department of Chemistry, Warsaw University of Technology, Noakowskiego 3, 00-664 Warsaw, Poland
[2]Institute of Organic Industrial Chemistry, Annopol 6, 03-236 Warsaw, Poland

Abstract

The mixing and melting enthalpy of the binary system nitrocellulose+2,6-dinitrotoluene was determined using the DSC method. The mixing enthalpy of the components was calculated. At the melting temperature the maximum value of the mixing enthalpy for the mole fraction x_{w26DNT}=0.607 is equal H_{max}^{M} = –3.41 kJ mol^{-1}. Measurements of the melting process (second measurement) were conducted after a storage period of several days at room temperature. Analysis of the melting peaks shows that the melting process of 26DNT takes place in pores of the micro-fiber and bulk outside the fibers. In the case of a mass fraction of x_{w26DNT}>0.9 the melting process takes place in the bulk, which suggests that in the case of such concentrations separation of the micro-fibers occurs.

Keywords: 2,6-dinitrotoluene, DSC, mixing enthalpy, nitrocellulose

Introduction

Nitrocellulose is a rigid polymer with a fibrous structure. It is not suitable for direct processing. To improve the properties of NC low-molecular compounds are introduced into its structure. This means to plastify NC or improve its chemical stability. The presence of a strong polar group (OH) and a less polar group (ONO$_2$) connected to the non-polar ring have a decisive influence on the physicochemical properties of NC. The NC chain forms a 5_2 type helix [1]. Baker's works [2], carrying over the similarity in the spatial structure of cellulose, suggest that NC consists of a two-dimensional table of 12×8 chains twisted in the form of a helix. Such a structure forms a micro-fiber. Micro-fibers form thin NC fibers in the shape of tubes.

2,6-Dinitrotoluene (26DNT) plays the role of NC plastifier and phlegmatization agent of the combustion process. Brodman's studies [3] conducted in IR spectra indicate the existence of weak hydrogen bonds between unestrified OH groups in NC and nitro groups in DNT. In paper [4] properties of hydrogen bonds in various isomers of DNT are compared. The hydrogen bond causes the nitro group to deviate from the plane of the aromatic ring. Winkler [5] applied the CNDO/2 method and confirmed

the existence of hydrogen bonds. The mean energy of reaction on the DNT particle is equal to 10 kcal mol^{-1}.

The aim of this study is to determine the mixing enthalpy based on the melting enthalpy of 26DNT in the mixture and to establish the structure change in the mixture by analyzing the melting process of the low-molecular compound. The mixing process of NC is complex. It consists of the following stages: wetting, swelling and displacement of the polymer chains into the dissolvent. In this paper we shall call the total thermal effect connected with the above mentioned stages the mixing enthalpy. The mixing enthalpy is the measure, of the intermolecular interactions within the mixture.

Experimental

In this study *NC* produced from wood in the ZTS 'Pronit' factory in Pionki, with a nitrogen content of 13.2% and number-average molecular mass of M_n=54·10^3 g mol^{-1}, was used. Before measurements were conducted NC was rinsed with distilled water for 24 h to remove impurities. Fully dried NC was then stored in a desiccator over P$_2$O$_5$.

26DNT exists in A and B form [6]. 26DNT was crystallized from acetone. Purity after crystallization determined by the cryometric method is equal 99.7%. The melting enthalpy of the A form is equal to ΔH_m=93.7 J g^{-1} and of the B form ΔH_m=121.0 J g^{-1}.

NC and 26DNT mixture was prepared through precise mixing of components and pressing under the pressure of 1 GPa for 1 min into pellets of dimensions resembling those of the calorimetric vessel. The sample was then closed in an aluminium vessel under the pressure of approximately 1.3 kPa. Measurements were conducted on a model Pyris-1 Perkin Elmer scanning microcalorimeter. The melting process was investigated with the heating rate of β=2 K min^{-1} and glass temperature with β=20 K min^{-1}.

Method background

It was assumed that the penetration of 26DNT into amorphous NC fibers starts at the beginning of the melting process of 26DNT during the first DSC measurements. Endothermic peaks observed in DSC curves are due to the melting of 26DNT and the molecular interaction between liquid 26DNT and NC chains. The contribution of 26DNT melting enthalpy per 1 g of the mixture can be predicted according to the relation:

$$\Delta H_{m26DNT} = \Delta H^0_{m26DNT} x_{w26DNT} \tag{1}$$

where ΔH^0_{m26DNT} is the melting enthalpy per 1 g of pure 26DNT, and x_{w26DNT} is the mass fraction of 26DNT in the investigated mixture. The enthalpy corresponding to the mixing (interaction) of 26DNT molecules with NC chains is given by:

$$H^M = \Delta H - \Delta H_{m(w26DNT)} \tag{2}$$

where ΔH is the experimental enthalpy for 26DNT melting and mixing processes per 1 g of mixture. For better discussion it is more convenient to express $\overline{H}^{M}$ per 1 mole of mixture as

$$\overline{H}^{M} = H^{M}[x_{26DNT}M_{26DNT} + (1 - x_{26DNT})M_{NC}] \tag{3}$$

where x_{26DNT} – mole fraction of 26DNT, M_{26DNT} – molecular mass of 26DNT, M_{NC} – molecular mass of unit (sub-mole nitrocellulose) which is a function of the average number (Y) of the groups attached to one anhydroglucose ring according to the formula: $(C_6H_7O_2)(OH)_{3-Y}(ONO_2)_Y$.

Results and discussion

26DNT achieves crystalline form (B) [6] with reversible and form A irreversible melting processes. The DSC curves are different, which renders identification easy. The melting process of 26DNT crystallized from acetone is irreversible. After melting and crystallization it forms crystals showing solid-solid phase transition and reversibility of the melting process of crystals B. DSC curves of the attained forms are shown in Fig. 1. The thin line represents the DSC melting curve of the irreversible melting process of form A. The determined melting temperature is equal to 331.0 K. The thick line represents the DSC curve consisting of two peaks: solid-solid transition at 323.0 K and reversible melting process at 341.0 K. It was noticed that pressing form B facilitates production of form A. Crystallized 26DNT was used to prepare the mixture. The achieved form was better suitable for attaining a more homogenized sample. Because both forms are easily discriminable, their presence was taken into account when calculating mixing enthalpy.
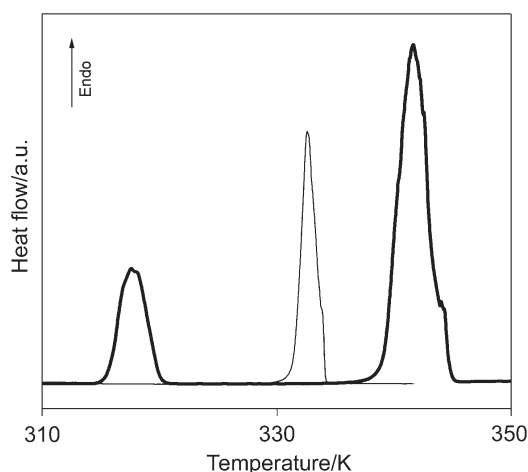
Fig. 1 DSC curve of the melting process and solid-solid transition for 2,6-DNT in form B (thick line) and irreversible melting process form A (thin line), with heating rate $\beta=2$ K min^{-1}

DSC measurements of melting and phase transition were conducted in the temperature range of 293–380 K. During the first measurements 26DNT was mixed with NC by melting fine powdered 26DNT with ground NC fibers. Figure 2 shows the DSC curve of the first measurement with mass fraction x_{w26DNT}=0.500 content. Endothermic peak (A) concerns solid-solid transition. It is followed by a small endothermic peak (B) connected with the melting of form A. Endothermic peak (C) concerns the melting of form B. This peak changes into exothermic peak (D) connected with the exothermic effect of the component mixing process.
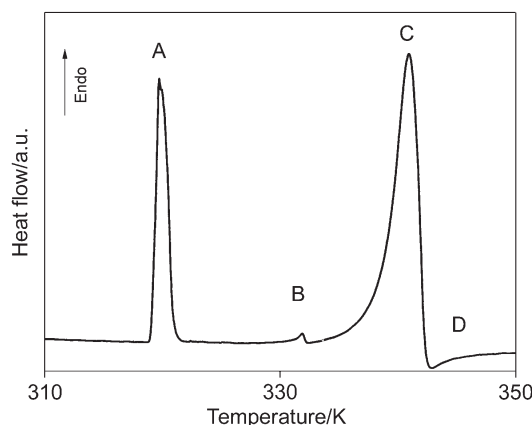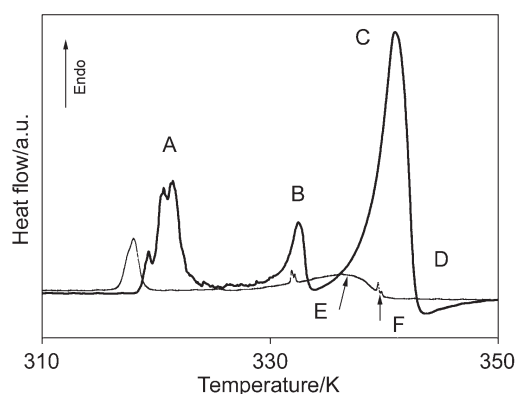

Fig. 2 DSC curve melting and mixing for x_{w26DNT}= 0.500 for the first measurement, with heating rate β=2 K min^{-1}

Taking into account the very high melting temperature of NC (extrapolated value is equal 890.20 K [7, 8]) and assuming that the components form a simple eutectic, its temperature will be close to the melting temperature of 26DNT. Below the eutectic temperature crystallization of 26DNT not bound with the NC chain takes place. Taking into account the slow manner in which thermodynamic equilibrium is established in the system under investigation, reheating of the sample during measurement will lead to the (bulk) melting of 26DNT at the melting temperature of pure 26DNT and melting in pores at lower temperatures. Lowering the temperature will be connected with the shape and dimensions of the pores between fibers [9].

Analysis of DSC curves of the mixture began at x_{w26DNT}=0.302, because in the case of lower mass fractions x_{w26DNT} the transition peaks on the DSC curves in subsequent measurements conducted on the same sample do not occur or can be disregarded. Such shapes of the curves suggest that 26DNT molecules are bound strongly with NC chains and do not undergo crystallization. Figure 3 shows DSC curves for a weight fraction of x_{w26DNT}=0.302. The same denotations are used as in Fig. 2. The first DSC measurement (thick line) and the second DSC measurement were conducted on the same sample. The second measurement was carried out after the sample had been stored at room temperature (approximately 293 K) for five days. The solid-solid transition (A) in the second measurement shifted toward lower temperatures by 4 K.

Melting of the form A, (peak (B)), takes place in the same temperature range in both measurements. The wide peak (E) in Fig. 3 is connected with the melting of form B in the pores (interfiberal). On the final segment of peak E an additional endothermic effect (F) is visible. This is connected with the melting of 26DNT in pores space most likely on the surface of NC fibers. The thermal effects of transitions in the second measurement are much smaller than in the first measurement. This is a result of stable associated molecules of 26DNT and NC chains forming. Small, acute peaks occurring in the melting temperature of pure 26DNT (for both form A and B) suggest that this is the bulk.
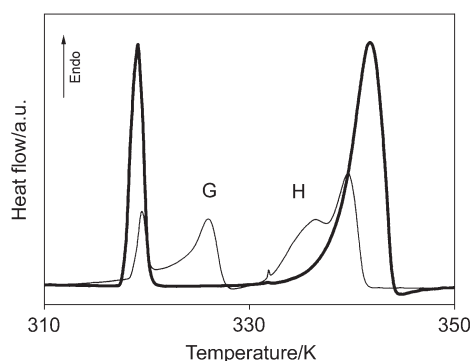
Fig. 3 DSC curve melting and mixing of the first measurement (thick line) and the phase transitions of the second measurement (thin line) performed with the sample x_{w26DNT}=0.302, with heating rate β=2 K min^{-1}
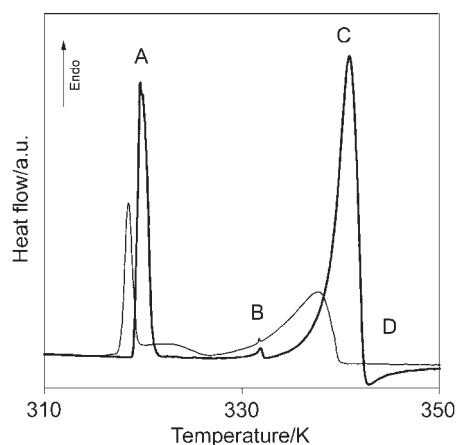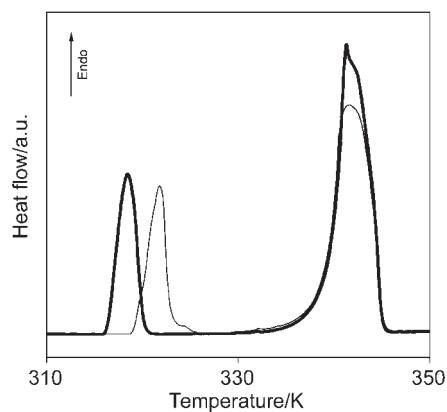
Fig. 4 DSC curve melting and mixing of the first measurement (thick line) and the phase transitions of the second measurement (thin line) performed with the sample x_{w26DNT}=0.500, with heating rate β=2 K min^{-1}

A similar course of the analogous curves can be observed for a mass fraction of $x_{w26DNT}=0.500$. This is illustrated in Fig. 4. In this case the peak connected with the melting of form A is very small both in the first and the second measurements. The DSC curve of the second measurement possesses a clearly changed base-line between peaks A and B, which suggests that melting of form A takes place in the non-limited space. In the second measurement the melting temperatures are shifted toward lower temperatures, which indicates that the low-molecular component crystallized in the limited space.

Fig. 5 DSC curves melting and mixing of the first measurement (thick line) and the phase transitions of the second measurement (thin line) performed with the sample $x_{w26DNT}=0.600$, with heating rate $\beta=2$ K min^{-1}

Fig. 6 DSC curves melting and mixing of the first measurements (thick line) and the phase transitions of the second measurement (thin line) performed with the sample $x_{w26DNT}=0.899$, with heating rate $\beta=2$ K min^{-1}

Figure 5 represents the DSC curves of subsequent measurements for $x_{w26DNT}=0.600$. The first measurement was carried out immediately after the mixture was prepared, the second four days later. The sample was stored in the hermetic pan between measure-

ments. After four days a thermal effect (G) appears on the DSC curve after the solid-solid transition. This is connected with the melting of form A in the limited space. Near point H melting of form B occurs in the pores with two discriminable parameters. This is due to the equilibrium of two various structures formed as a result of NC–26DNT interaction.

On the DSC curve for x_{w26DNT}=0.898 (Fig. 6) thermal effects of the melting process of form A are very small in the first and in the second measurement, which was carried out 105 min later. For samples of low 26DNT content applying pressure while pressing the samples (thick line) produces an effective transition (thin line) from form A to B. Good conformity of the melting temperatures of 26DNT and the shape of the initial segment of the DSC curve in the first and second measurement suggest that in the case of such a concentration separation of micro-fibers takes place. This is the reason why crystallization occurs only in the non-limited space.
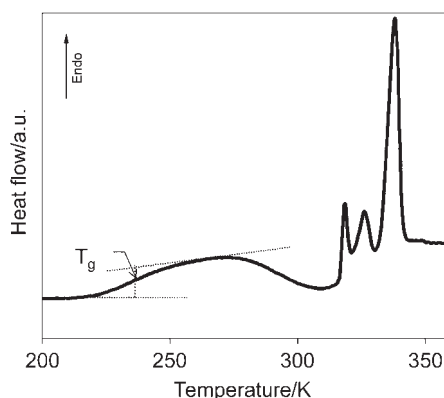

Fig. 7 DSC curve of phase transitions for x_{w26DNT}=0.500 with heating rate β=20 K min^{-1}

Measurements of the glass temperatures (T_g) of the samples stored in room temperature were conducted. The sample was heated with a rate of β=20 K min^{-1} up to 380 K, then it was cooled down at the same rate to 173 and after 1 min it was heated at the same rate to 380 K. The DSC curve for x_{w26DNT}=0.500 of the final stage is presented in Fig. 7. The vitrification temperature for this fraction is equal to T_g=234.0 K and is not significantly higher than the glass temperature of the pure component T_g=230.0 K. This conformity shows that 26DNT does not form stable amorphous solid solution with NC. The insignificant increase of T_g compared to the pure component is connected with the gradual solution of NC in 26DNT during measurement. Lack of glass transition of the samples stored for extended periods of time at room temperature confirms the above-mentioned assumptions. At higher temperatures the curve is more complex. It consists of a wide exothermic peak connected with crystallization and subsequent three peaks connected with melting in the pores and non-limited space (bulk).

During the estimation of the mixing enthalpy based on Eqs (1)–(3) different values of melting enthalpy of forms A and B were taken into account. Negative values of the mixing enthalpy in the whole range of concentrations are evidences of the interac-

tion between 26DNT molecules and NC chains. The melting enthalpy ΔH_m in the first measurement and the mixing enthalpies H^M calculated based on it are gathered in Table 1 in columns 3 and 2 respectively. The maximum measured value of the mixing enthalpy is equal $\overline{H}^M_{max}$ –3.41 kJ mol^{-1} for a mass fraction of x_{w26DNT}=0.607. In the previous work [10] the mixing enthalpy of the NC+s-diethylphenylurea (C1) was determined in a similar manner. The maximum mixing enthalpy was equal to $\overline{H}^M_{max}$= –4.59 kJ mol^{-1} for x_{C1}=0.555. These results show that C1 is a better solvent for NC.

Table 1 Mixing enthalpy of the binary system nitrocellulose+2,6-dinitrotoluene at the melting temperature of 2,6-dinitrotoluene T_m=341.0 K

x_{wDNT}	$-H^M$/kJ mol^{-1}	ΔH_m/J g^{-1}
0.9510	0.39	86.99
0.8983	0.56	81.20
0.7012	2.00	55.87
0.5992	1.97	46.87
0.5000	3.41	31.37
0.4274	2.81	27.75
0.3015	1.53	21.93
0.2164	0.36	18.84
0.1171	0.17	10.35
0.0483	0.28	3.51

Conclusions

Analysis of the position of the melting peak of 26DNT allows to draw the conclusions as to the structural changes in NC in samples stored at room temperature. At this temperature crystal of 26DNT is the stable form. This has been confirmed by measurements carried out in the temperature range of 173–380 K. Analysis of melting curves for x_{w26DNT}<0.3 shows that 26DNT is strongly bound with NC chains (lack of crystallization). For mixtures in the range of 0.3–0.9 crystallization occurs mainly in the space limited by NC chains pores. The melting temperature of 26DNT is lower than the melting temperature of the pure component. For mass fractions of x_{w26DNT}>0.9 the melting temperature of pure 26DNT and the mixture are conforming, which suggests that crystallization occurs in the non-limited space (bulk). The established mixing enthalpy is negative (exothermic effect), which indicates strong interaction between liquid 26DNT with NC chains.

* * *

References

 1 D. Meader, E. D. T. Atkins and F. Happey, Polymer, 19 (1978) 1371.
 2 F. S. Baker and G. J. Privett, Polymer, 28 (1987) 1121.
 3 B. W. Brodman, N. Lampner and M. P. Devine, J. Appl. Polym. Sci., 26 (1981) 1739.
 4 B. W. Brodman and N. Lampner, J. Appl. Polym. Sci., 27 (1982) 3621.
 5 D. A. Winkler, Polymer Communications, 30 (1989) 50.
 6 A. Finch and J. Payne, Thermochim. Acta, 164 (1990) 55.
 7 S. Newman, J. Polym. Sci., 13 (1954) 179.
 8 P. J. Flory, R. R. Garrett, S. Newman and L. Mandelkern, J. Polym. Sci., 12 (1954) 97.
 9 L. G. Homshaw, J. Colloid Interface Sci., 84 (1981) 127.
10 A. Książczak and T. Książczak, J. Therm. Anal. Cal., 54 (1998) 323.